ELSEVIER

Ceramics International 33 (2007) 123–132

CERAMICS
INTERNATIONAL

www.elsevier.com/locate/ceramint

Synthesis of low expansion ceramics in lithia–alumina–silica system with zirconia additive using the powder precursor in the form of hydroxyhydrogel

S. Mandal, S. Chakrabarti, S.K. Das *, S. Ghatak

Clay & Traditional Ceramics Division, Central Glass & Ceramic Research Institute, 196,
Raja S.C. Mullick Road, P.O. Jadavpur University, Kolkata 700 032, India

Received 31 May 2005; received in revised form 17 June 2005; accepted 24 August 2005
Available online 15 December 2005

Abstract

Powder precursors lithium aluminosilicate (LAS) of low expansion characteristics were synthesized by following the wet interaction technique in the hydroxyhydrogel form using lithium carbonate (Li_2CO_3), hydrated aluminium nitrate [$Al(NO_3)_3 \cdot 9H_2O$], fume silica (SiO_2) and zirconium oxychloride ($ZrOCl_2 \cdot 8H_2O$). Dilatometry, X-ray diffraction (XRD), IR analysis, Scanning Electron Microscopy (SEM) and Image analysis were done to study sintering, characteristics phase transformation and microstructure on the sintered specimens. ZrO_2 was found to promote the formation of β-eucryptite, and grain size of the sintered specimens could be related to the amount of ZrO_2 present in the starting powder precursor. The thermal expansion characteristics were also found to be strongly influenced by ZrO_2 content in the specimens.

Keywords: Low expansion ceramics; $Li_2O–Al_2O_3–SiO_2$; Powder precursor; Hydroxyhydrogel; β-eucryptite

1. Introduction

Low expansion ceramics are used in electronic devices, cookware, in precision parts of heat engines components and spark plugs [1,2] and also have been widely used in the glass and ceramic industry as lithia-bearing fluxes and low-expansion fillers in white-ware bodies [3,4]. It has been known that thermal shock resistance of ceramics is influenced by the thermal expansion coefficient especially when the rate of heat transfer of the ceramics in question is large. The interesting properties of such materials are mainly attributed to their crystal structures, which consists of flexible and strongly bonded three-dimensional networks developing a rigid stable hexagonal lattice containing structural holes or interstices which can be partially or fully occupied by several ions such as Na^+, Li^+, Ca^{++}, Sr^{++}, and Ba^{++} [5].

The important crystalline phases present in $Li_2O–Al_2O_3–SiO_2$ system include β-eucryptite ($Li_2O \cdot Al_2O_3 \cdot 2SiO_2$), β-spodumene ($Li_2O \cdot Al_2O_3 \cdot 4SiO_2$), virgilite ($Li_2O \cdot Al_2O_3 \cdot 6SiO_2$), petalite ($Li_2O \cdot Al_2O_3 \cdot 8SiO_2$) as well as metastable solid solutions [6] that are derived from the hexagonal high quartz structures by the substitution of Al^{3+} and Li^+ for Si^{4+}. These solid solutions are denoted as β-quartz (ss) and have the general compositions $Li_2O \cdot Al_2O_3 \cdot nSiO_2$, where n varies from 2 to 10 [7,8]. Table 1 [9–13] shows the list of materials based on lithium aluminosilicate (LAS) family known to have negative to zero to positive coefficient of thermal expansion (α) over a temperature range.

Yang et al. [6] reported that on heating the lithium aluminosilicate gel monoliths derived by sol–gel technique, β-eucryptite crystals were first precipitated at around 750 °C, followed by precipitation of β-spodumene crystals at 830 °C. He observed that at higher temperatures the latter grew at the expense of the former phase. The crystallized specimens exhibited very low thermal expansion coefficient ranging from -13 to $+12 \times 10^{-7}$/°C at temperatures from room temperature to 700 °C depending on the heat treatment temperature of the gels. Large glass ceramic monoliths in the system $Li_2O–Al_2O_3–SiO_2$ was prepared by Orcel and Hench [14] with the help of drying control chemical additives (DCCA). Wang et al. [15] reported

---

* Corresponding author. Tel.: +91 33 24733496; fax: +91 33 24730957.
E-mail address: swapan@cgcri.res.in (S.K. Das).

0272-8842/$32.00 © 2005 Elsevier Ltd and Techna Group S.r.l. All rights reserved.
doi:10.1016/j.ceramint.2005.08.015

Table 1
Average linear thermal expansion of some important materials based on lithium aluminosilicate (LAS) family [9–13]

System/material	Coefficient of thermal expansion ($^\circ C^{-1} \times 10^{-7}$)
β-Eucryptite (LAS 1:1:2), LiAl[SiO_4]	(−) 64 and (−) 86
β-Spodumene (LAS 1:1:4), LiAl[Si_2O_6]	(+) 9 and (+) 12
Virgilite (lithium orthoclase) (LAS 1:1:6), LiAl[Si_3O_8]	(+) 5
Petalite (LAS 1:1:8) LiAl[Si_4O_{10}]	(+) 3
Solid solution of SiO_2 in β-eucryptite (LAS 1:1:3)	Small contraction (negative coefficient of expansion)
Solid solution of SiO_2 in β-eucryptite (LAS 1:1:3.5)	Zero thermal expansion
Pyroceram (LAS + TiO_2)	(−) 0.7 to (+) 13
Cer-vit (LAS + TiO_2 + ZrO_2)	(+) 0.5 to 3
Hercuvit (LAS-based transparent low expanding glass-ceramic)	0 to 3

that the solid LAS_4 precursor powders in this system wet each other due to a sufficient amount of the liquid phase and hence it was possible to obtain a densified sample with the addition of LiF as sintering aids [15]. He reported that precursor powder exhibited appreciable grain growth and the grain size varied from 1.0 to 25 μm with a non-uniform distribution resulting in discontinuous grain growth. In another study [16], it was reported that the grain size grew from 8 to 25 μm with a remarkable discontinuous grain growth of β-spodumene when sintered at 1050 °C for 5 h. The coefficient of thermal expansion of the sintered bodies decreased from 8.3 to $5.2 \times 10^{-7}/^\circ C$ (25–900 °C) as the LiF addition increased from 0 to 5 wt.%. The crystalline phases identified were a combination of β-eucryptite and eucryptite of different crystalline geometry. Beall [17] reported that extremely efficient nucleation was achieved in lithium aluminosilicate glasses by additions of TiO_2 and ZrO_2 in roughly equivalent molar concentrations of about 4 mol%. With this addition, it was possible to obtain a highly crystalline microstructure after heat treatment at 850 °C and the resulting glass ceramic yielded a single-phase material and had a coefficient of thermal expansion of up to $7 \times 10^{-7}/^\circ C$ (0–500 °C) and thus it produced outstanding thermal shock resistance. Abdel-Fattah and Abdellah reported [18] the values of negative and positive coefficient of linear thermal expansion of three different samples, sintered at different temperatures, as (−) $14.7 \times 10^{-7}/^\circ C$ (75–150 °C), (−) $8 \times 10^{-7}/^\circ C$ (75–150 °C) and (−) $1.3 \times 10^{-7}/^\circ C$ (75–150 °C) and (−) $23.7 \times 10^{-7}/^\circ C$ (500–575 °C), (+) $24 \times 10^{-7}/^\circ C$ (500–575 °C), (+) $32 \times 10^{-7}/^\circ C$ (500–575 °C), respectively, prepared by solid–solid interactive method in the system LiO_2–Al_2O_3–SiO_2. Wang [19] mentioned that at 800 °C the crystalline phase comprised the major phase of β-spodumene ($Li_2O{\cdot}Al_2O_3{\cdot}4SiO_2$) and the minor phase of β-eucryptite ($Li_2O{\cdot}Al_2O_3{\cdot}2SiO_2$). After calcinations at 1000 and 1200 °C, the XRD patterns showed pronounced growth of β-spodumene. The diffraction lines of β-eucryptite disappeared at 1200 °C.

It appears from the above discussion that tailoring of composition may produce sintered materials of desired thermal expansion characteristics. This tailoring is possible either by adjusting the composition to synthesize biphasic material or the composition may be selected in such a way that a phase transition is effected during the densification producing desired phases to manifest desired thermal expansion. In all the previous works of other authors, the initial composition comprised of lithium oxide, alumina and silica that produce mostly β-eucryptite, β-spodumene and phases consisting of lithiumaluminate spinel, lithiumaluminate, corundum and combination thereof. Formation and separation of such phases requires considerable higher processing temperature and as a consequence controlling the processing parameters become more complex. In addition, the above formation and segregation of undesirable phases exerts undesirable influence on the desired properties. These difficulties or drawbacks may be overcome by taking broadly two measures namely (i) appropriate processing of right type of raw materials to make powder precursor in the form of hydroxyhydrogel [20–23] which on further processing gives the desired product. This may be carried out by forming a hydroxyhydrogel type of intermediate powder precursor [24] in the system Li_2O–Al_2O_3–SiO_2; and (ii) using a nucleating material which catalyses the formation of desirable phase in the sintered composites exhibiting low thermal expansion in the desired temperature range.

The present investigation was undertaken to synthesize powder precursor of lithium aluminosilicate by following wet interaction technique [24]. The sintering characteristics of the powder precursors were characterized by the thermal analysis, IR spectroscopy and microstructural analysis. The effect of ZrO_2 on the phase formation was analysed with respect to various physicochemical parameters.

2. Experimental

2.1. Preparation of lithium aluminosilicate hydroxyhydrogel as powder precursor

Powder precursors in the form of hydroxyhydrogel of composition LAS 1:1:2 in the system LiO_2–Al_2O_3–SiO_2 were prepared by wet interaction in aqueous medium by flash poly-

Table 2
Oxide composition (wt.%) of powder precursors of lithium aluminosilicate (LAS) hydroxyhydrogel before and after calcinations at 750 °C

Constituents	Before calcinations	After calcinations	Sample number
Li_2O	11.86	10.54	Sample I → LAS +
Al_2O_3	40.46	36.21	0.00 wt.% ZrO_2,
SiO_2	47.68	53.25	Sample II → LAS +
ZrO_2 (extra addition per 100 gm of batch)	0.00	0.00	4.0 wt.% ZrO_2,
			Sample III → LAS +
	4.00	2.46	6.0 wt.% ZrO_2,
	6.00	3.05	Sample IV → LAS +
	8.00	5.32	8.0 wt.% ZrO_2

condensation technique [24] using LR grade lithium carbonate (Li_2CO_3), hydrated aluminium nitrate [$Al(NO_3)_3 \cdot 9H_2O$], fumed silica (SiO_2) and zirconium oxychloride ($ZrOCl_2 \cdot 8H_2O$) as a source of LiO_2, Al_2O_3, SiO_2 and ZrO_2, respectively. Calculated quantity of lithium carbonate was first added to a measured volume of distilled water, stirred and boiled for 5 min. The pH of the aqueous lithium carbonate was adjusted to acidic pH by gradual addition of nitric acid till effervescence was ceased (Solution A). A calculated quantity of LR grade hydrated aluminium nitrate was dissolved in measured quantity of distilled water to make a clear solution and then it was added into the solution marked 'A' with stirring till complete dissolution into the lithium nitrate solution (Solution B). Weighed quantity of zirconium oxychloride was dissolved in measured quantity of distilled water to make a clear solution. It was added gradually into the Solution B with stirring (Solution C). Weighed quantity of fumed silica (Cab-O-Sil make, M/s Vaunam Agencies, Kolkata) was added into the mixed solution marked 'C' with continuous stirring to obtain a suspension. The suspension so prepared was poured into calculated amount of 25% ammonia solution under stirring so that the pH of the mixture after the reaction remains between 5 and 7. The entire mixture took the consistency of a thick gel like mass. The gel like mass was kept at room temperature for 24 h followed by evaporation to dryness with occasional stirring. The resultant powder precursors so prepared have been classified as batches I, II, III and IV depending upon the amount of ZrO_2 content. The powder precursors of different batches were then dried at 110 ± 5 °C and were calcined at 750 °C for 2 h. The contents of LiO_2, Al_2O_3, SiO_2 and ZrO_2 after calcinations were analyzed chemically. The composition of batches I–IV including the ZrO_2 content and the analyzed composition of the different batches are shown in Table 2.

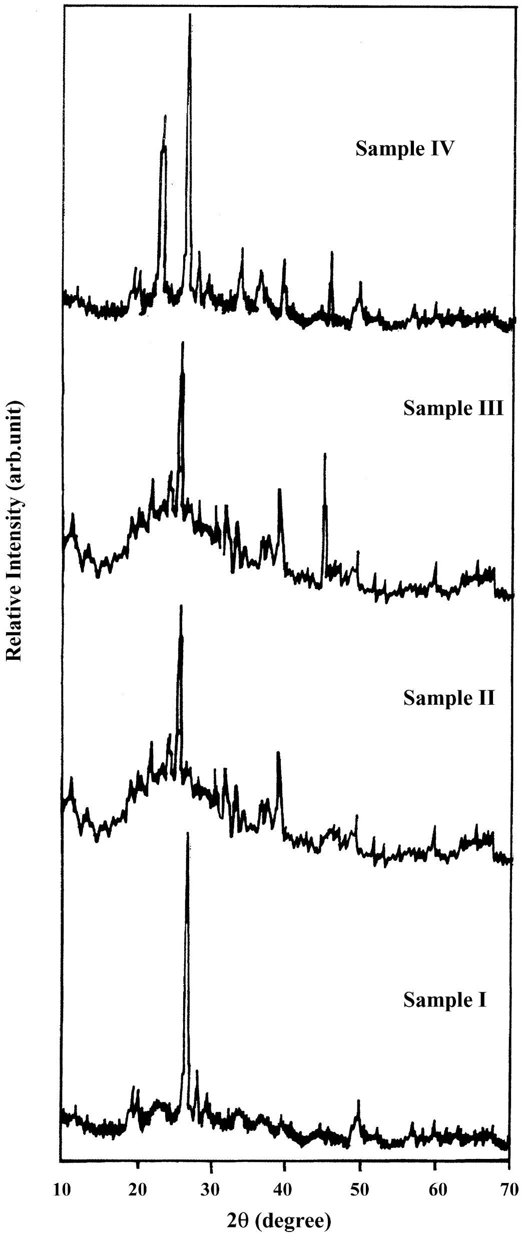

Fig. 1. XRD patterns of the hydroxyhydrogel precursor powders calcined at 750 °C.

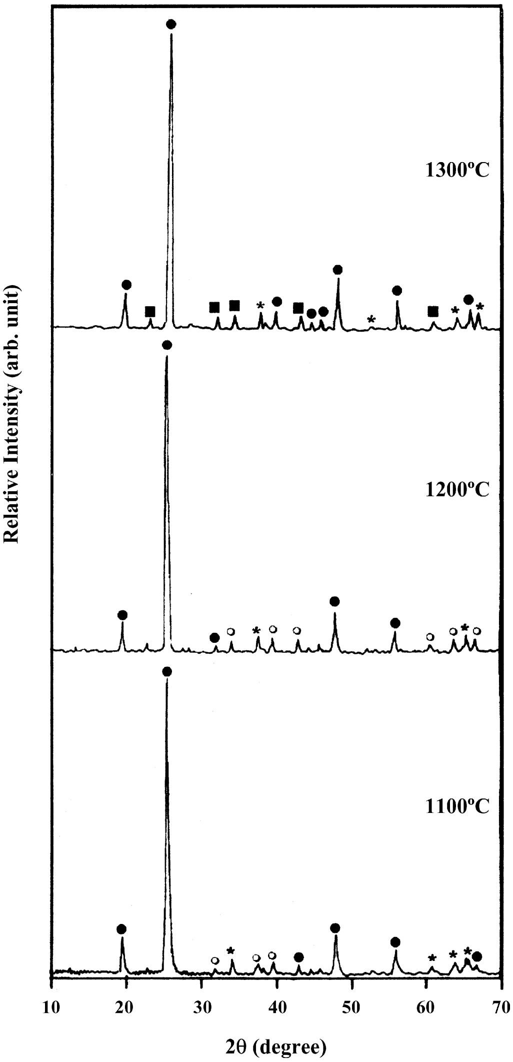

Fig. 2. XRD patterns of the sample I heat treated at different temperatures.(●) Lithium aluminium oxide [$LiAl_5O_8$; PDF# 38-1425]; (*) Lithium aluminosilicate [$LiAlSi_2O_6$; PDF# 35-0797]; (○) Lithium aluminosilicate [$Li1.01(Al_2O_3)1.03(SiO_2)1.16$; PDF# 45-0467; and (■) Silicon Oxide (SiO_2) [PDF# 27-0605].

2.2. Preparation of test specimen and sintering

The calcined mass was ground and sieved to pass through 100 mesh B.S. The test specimens were prepared in the form of rectangular bars of dimension 60 mm × 10 mm × 8 mm by uni-axially pressing at 25 MPa followed by cold iso-static pressing at 200 MPa. Sintering experiments were carried out by heating at 1100, 1200, 1300 and 1350 °C in an electric furnace in ambient atmosphere with 2 h soaking at the respective peak temperatures.

2.3. Measurement of thermal expansion

The sintered specimens for the thermal expansion experiment were cut into bars of dimension 25 mm × 6 mm × 6 mm. The thermal expansion of the specimens was determined in the temperature range 30–800 °C using push rod type Orton Dilatometer (Model 1500D) at heating rate of 10 °C/min in ambient atmosphere.

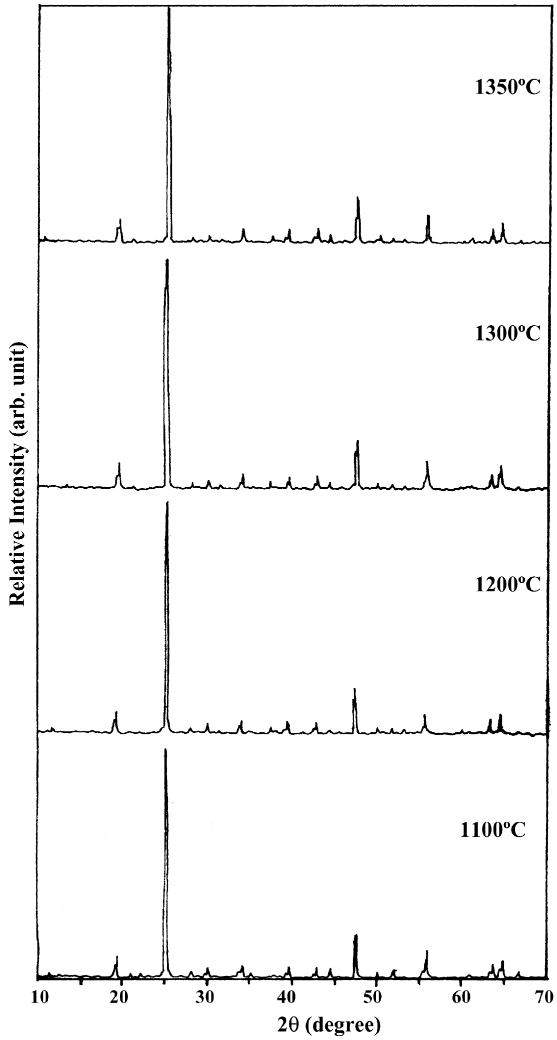

Fig. 3. Representative XRD pattern of the processed Lithia–alumina–silica–zirconia hydroxyhydrogel heat treated at different temperatures.

2.4. IR analysis

FTIR of the samples heat treated at 1300 °C was performed with Perkin–Elmer model no. 1615 FTIR spectrometer using KBr pellete technique in the wave number range 400–4000 cm^{-1}.

2.5. XRD analysis, microstructural studies and image analysis

The XRD studies for all the samples heat treated at different temperatures were carried out using a Philips PW-1730 with Cu Kα radiation and Ni filter. The microstructural analysis of the samples I–IV heat-treated at 1100 and 1300 °C were also examined by Scanning Electron Microscopy (LEO 430i, UK) operated at an accelerating voltage of 10 kV. The image analysis of the SEM photographs of the heat-treated samples was done using Leica-Q500 MC software.

3. Results and discussion

The XRD patterns of the hydroxyhydrogel powders (samples I–IV) when calcined at 750 °C are shown in Fig. 1. It is clear from the figure that lithium aluminosilicate (β-eucryptite) formed at 750 °C for all except sample I (without the additive) [25]. The XRD patterns of sample I heat-treated in the temperature range between 1100 and 1300 °C are shown in Fig. 2, where the different phases formed in the sample after sintering at different temperatures were lithium aluminosilicate (β-spodumene) ($LiAlSi_2O_6$), lithium aluminiumoxide ($LiAl_5O_8$) and silicon oxide (SiO_2) and trace amount of lithium aluminosilicate (β-eucryptite) ($LiAlSiO_4$) in varying

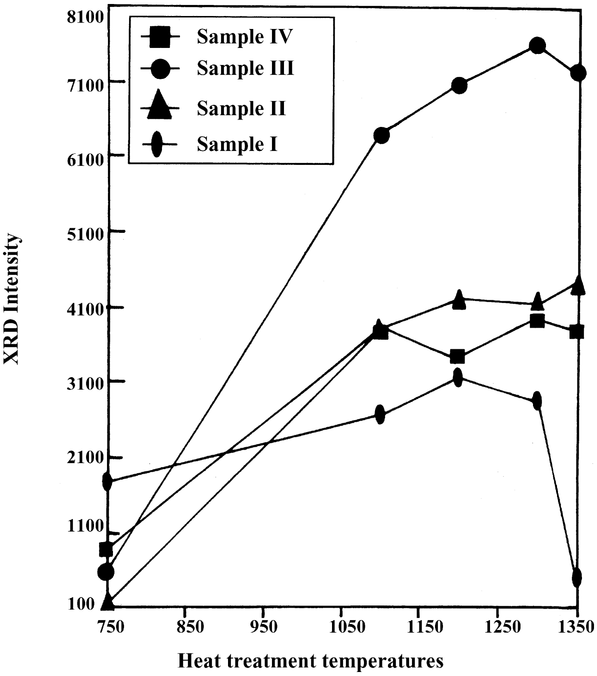

Fig. 4. Behavior of 102 peak intensity [samples II, III and IV] and 311 peak intensity [sample I] with respect to heat treatment temperatures.

amounts, the amount of which was found to be increasing with increasing sintering temperature. But in the case of samples II–IV, lithium aluminosilicate (β-eucryptite) crystalline phase ($LiAlSiO_4$) was formed as a single major phase at all sintering temperature. However, the reflections of other minor associated phases (in trace amounts) were also noticed as detected from their intensities of XRD files. One representative XRD pattern of the processed lithia–alumina–silica–zirconia hydroxyhydrogel heat treated at different temperatures between 1100 and 1350 °C showing the formation of β-eucryptite is shown in Fig. 3. The maximum peak intensity of the crystalline phase-like β-eucryptite for samples II–IV and lithium aluminium-oxide for sample I [25] formed was plotted against the different heat treatment temperatures and is shown in Fig. 4. It is observed from this figure that 102 (PDF# 17-534) Peak intensity of the β-eucryptite phase was achieved for the samples II–IV when heat-treated at 1100 °C and thereafter the intensity increased with varying magnitudes. On the other hand, the 311 (PDF# 38-1425) Peak intensity of lithium aluminiumoxide crystalline phase (sample I) was consistently lower than the other specimens. The intensity of the phases appeared in sample I drastically reduced to a much lesser extent at 1350 °C which might be due to the initiation of vitrification. Therefore, it can be said that almost complete reaction towards the formation of β-eucryptite phase was noted for samples II–IV sintered at 1100 °C (Fig. 4). Hence, it may be inferred that zirconia had a dominating influence towards the formation of β-eucryptite in the present system. The formation of β-eucryptite in the present

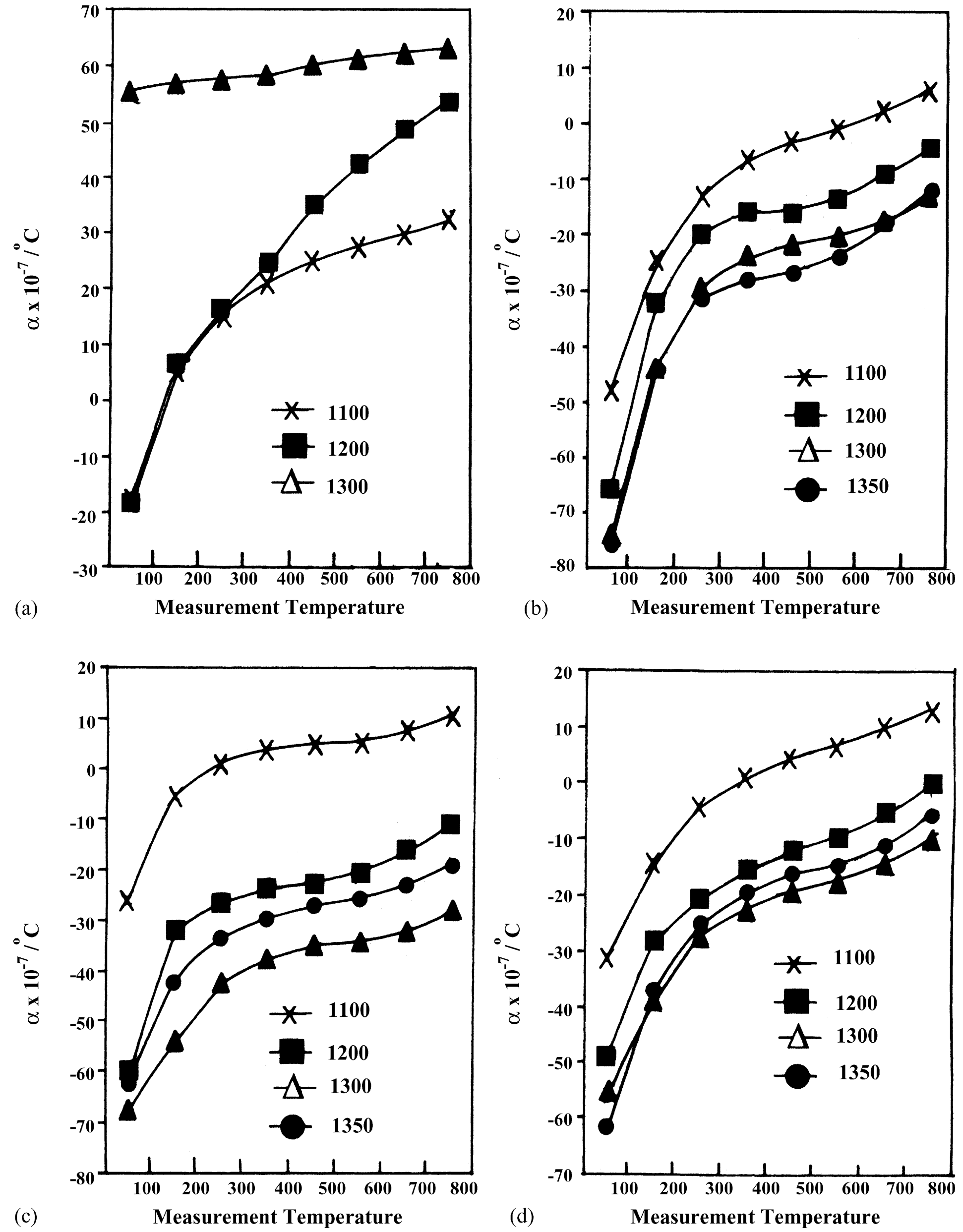

Fig. 5. Thermal expansion behavior of the samples [a: sample I, b: sample II, c: sample III and d: sample IV] heat treated at different temperatures in relation to the temperature of measurement.

Table 3
Coefficient of thermal expansion values (CTE × 10^{-7}/°C) of the reaction sintered specimens heat treated at 1100, 1200, and 1300 °C

Sample number	Coefficient of thermal expansion values (CTE × 10^{-7}/°C) of the samples			
	$\alpha \times 10^{-7}$/°C (RT-800 °C) sintering temperature: 1100 °C	$\alpha \times 10^{-7}$/°C (RT-800 °C) sintering temperature: 1200 °C	$\alpha \times 10^{-7}$/°C (RT-800 °C) sintering temperature: 1300 °C	$\alpha \times 10^{-7}$/°C (RT-800 °C) sintering temperature: 1350 °C
I	−17.2 to 31.5	−18.7 to 53.7	55.6 to 63.9	Sample deformed
II	−48 to 6.35	−65.5 to −3.95	−75.4 to −11.8	−74 to −12.7
III	−26 to 10.8	−60 to −10.7	−61.9 to −18.5	−67 to −27.6
IV	−31.4 to 12.9	−49 to −8.05	−61.6 to 5.51	−55.8 to −9.90

system was further supported by the thermal expansion values as shown in Table 3 and Fig. 5. Sample I heat-treated at 1100 and 1200 °C showed negative expansion up to 150 °C followed by positive expansion and when further heat-treated at 1300 °C the sample showed high positive expansion values. Sample II showed negative to positive expansion when heat-treated at 1100 °C and similar trend was noted for samples III and IV. On the other hand, samples II–IV showed only negative expansion when heat treatment temperature was raised to 1200, 1300 and 1350 °C. Therefore, it may be said that ZrO_2 promoted the formation of β-eucryptite and consequently thermal expansion characteristics was found to be strongly influenced by ZrO_2 present in the starting powder precursor.

The general features of the microstructure of the samples heat-treated at 1100 and 1300 °C are shown in Fig. 6A–F. A detailed analysis of the microstructure by image analysis (Tables 4a and b) as well as visual observation indicated the presence of larger grains in sample I (Fig. 6A and B) when sintered at 1100 and 1300 °C. For samples II–IV, majority of the grains were below 5 μm (sintered at 1100 °C) (Table 4a and Fig. 6C and E). When the sintering temperature was raised to 1300 °C, a general grain growth was noted for all the samples

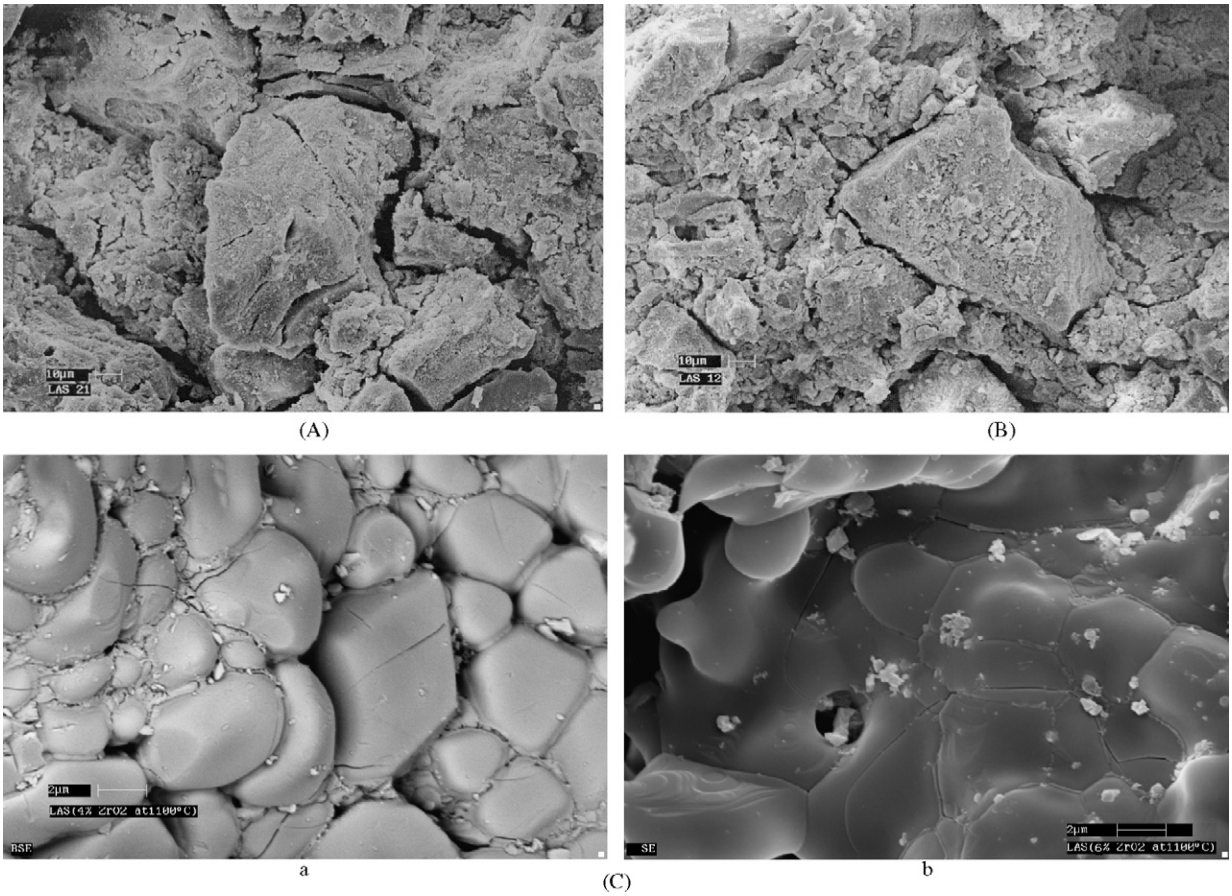

(A) (B)

a b

(C)

Fig. 6. (A) SEM photograph of sample I heat treated at 1100 °C. (B) SEM photograph of sample I heat treated at 1300 °C. (C) SEM photograph of the samples heat treated at 1100 °C (a: sample II, b sample III). (D) SEM photograph of the samples heat-treated at 1300 °C (c: sample II, d: sample III). (E) SEM photograph of sample IV heat treated at 1100 °C. (F) SEM photograph of sample IV heat treated at 1300 °C.

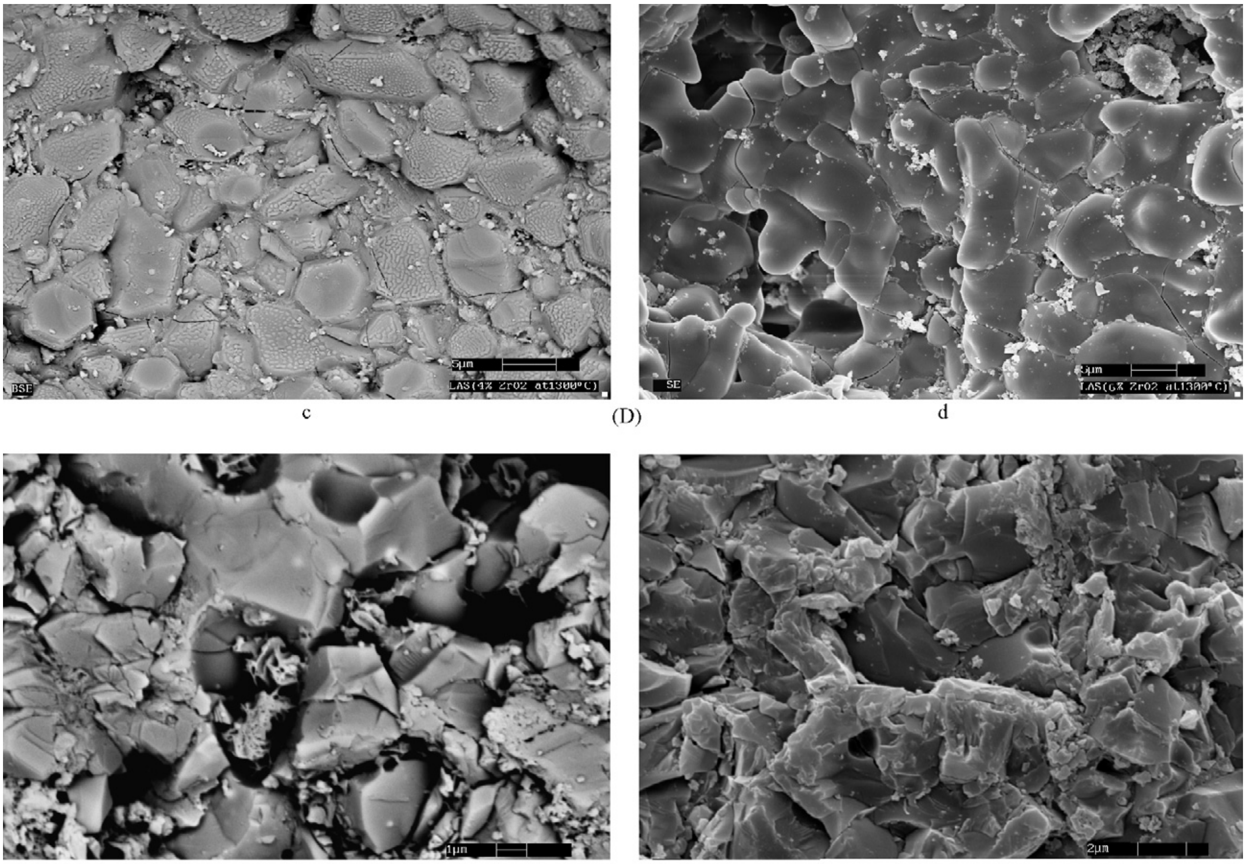

c (D) d

(E) (F)

Fig. 6. (*Continued*).

(Table 4b and Fig. 6B and D) excepting sample IV, where there was a general reduction in grain size [Table 4b and Fig. 6F]. However, the grain growth was more for sample I than other three samples (containing ZrO_2). Moreover, the tendency of grain growth decreased with increasing ZrO_2 content and ultimately for sample IV containing 8% ZrO_2 (Tables 4a and 4b, Fig. 6E and F), grain size was effectively reduced instead of a growth. Therefore, it may also be inferred that ZrO_2 not only induces the formation of β-eucryptite but also influences grain size.

This striking property of the materials in the present system might be due to the nature of powder precursors where Zr^{4+}, Si^{4+}, Al^{3+} and Li^{+} are present in a complex hydroxyhydrogel form in which those species occupy the preferred position in the desired orientation. The powder precursors were prepared by following wet interaction technique in aqueous medium. If aluminium salt is dissolved in aqueous medium, it forms an aquo complex $[Al(OH_2)_6]^{3+}$, water of which was gradually replaced by OH^- ions during reaction with hydroxide and polymerization proceeds with the formation of polynuclear complexes as described [26,27]. Similarly, reactive silica and zirconium salt also form respective aquo complexes with respective co-ordination number. The aquo complexes so

Table 4a
General feature of microstructure of the samples sintered at 1100 °C

Sample number	Area (%)	Aspect ratio of grains	Equivalent diameter (μm)	Percentage of grains of less than (μm)								
				5	10	20	30	40	50	60	70	80
I (10 μm)	78.59	1.15–2.35 (S.D. = 0.339, S.E. = 0.085)	Mean = 41.52, 18.01–74.27 (S.D. = 15.89, S.E. = 3.97)	None	None	12.5	12.5	31.25	12.50	18.75	6.25	6.25
II (2 μm)	81.57	1.10–2.65 (S.D. = 0.351, S.E. = 0.059)	1.78–7.82 (S.D. = 1.414, S.E. = 0.239)	85.71	14.29	–	–	–	–	–	–	–
III (2 μm)	81.64	1.13–3.00 (S.D. = 0.52, S.E. = 0.10)	1.85–7.79 (S.D. = 1.44, S.E. = 0.28)	73.08	26.92	–	–	–	–	–	–	–
IV (1 μm)	83.30	1.11–4.21 (S.D. = 0.69, S.E. = 0.13)	1.51–6.65 (S.D. = 1.51, S.E. = 0.28)	73.33	26.67	–	–	–	–	–	–	–

S.D.: standard deviation; S.E.: standard error.

Table 4b
General feature of microstructure of the samples sintered at 1300 °C

Sample No.	Area (%)	Aspect ratio of grains	Equivalent diameter (μm)	Percentage (%) of grains of less than (μm)									
				5	10	20	30	40	50	60	70	80	90
I (10 μm)	29.13	1.11–2.39 (S.D. = 0.288, S.E. = 0.052)	14.90–85.13 (S.D. = 13.07, S.E. = 2.35)	None	None	25.80	41.90	22.58	6.45	–	–	–	3.22
II (5 μm)	28.79	1.09–3.04 (S.D. = 0.42, S.E. = 0.05)	1.84–10.86 (S.D. = 1.94, S.E. = 0.24)	44.62	55.38	–	–	–	–	–	–	–	–
III (5 μm)	41.29	1.05–2.86 (S.D. = 0.35, S.E. = 0.05)	3.70–12.39 (S.D. = 1.93, S.E. = 0.26)	20.00	72.73	7.27	–	–	–	–	–	–	–
IV (2 μm)	38.60	1.10–2.95 (S.D. = 0.37, S.E. = 0.05)	1.14–5.12 (S.D. = 0.83, S.E. = 0.10)	100	–	–	–	–	–	–	–	–	–

S.D.: standard deviation; S.E.: standard error.

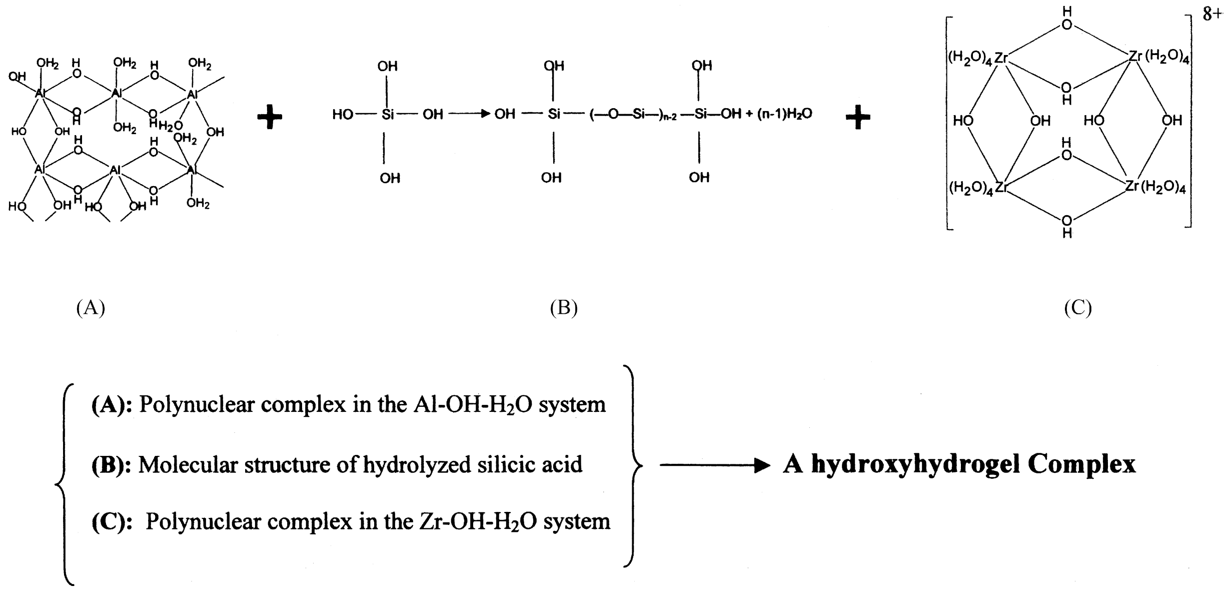

Fig. 7. Alumina–silica–zirconia acqo complexes forming a hydroxyhydrogel type network.

formed may be depicted as in Fig. 7 (zirconia–silica–aluminium–aquo complexes). If a mixture of those materials is polymerized by adjusting pH of the medium, these mixed cations are expected to be polymerized in such a way that the minimum free energy requirement is satisfied, as has been observed and published [28]. When silica and alumina form a polymeric network, the other cations, if present in smaller amount, will occupy the position in the network of polynuclear hydroxyhydrogel complex and will lead to a zeolitic structure. The zeolitic structure in turn has their intrinsic cavities and channels with ion exchange capabilities to hold other cations such as Li^+ in the present system. Zr^{4+} with ionic radius 0.80 Å may replace some of the Si^{4+} of radius 0.41 Å making the structure highly deformed. This process may take place without the requirement of charge neutralization as is required for the replacement of Si^{4+} by Al^{3+}. Though the metastability field of β-eucryptite solid solution is confined to the range of compositions 1:1:1 to about 1:1:1.60 (Li:Al:Si) [29] almost pure β-eucryptite was found to be formed in the present system which is in conformity to an early observation [30] where the transformation of β-quartz solid solution to β-spodumene solid solution in glass–ceramic system was found to be inhibited. During dehydration and dehydroxylation of the powder precursors, Zr^{4+} will reduce its co-ordination number from 8 to 7 [31] to accommodate itself in the polynuclear structure, though it has a large ionic radius in comparison to host cation. During dehydration or after dehydration and dehydroxylation, the cationic polynuclear structure though expected to be only oxo-linked, the IR results (Fig. 8) indicated the presence of residual hydroxy linkages. This metastable structure is prone to convert directly to a crystal such as β-eucryptite as was found in the present investigation.

4. Conclusions

Lithium aluminosilicate powder precursor in the hydroxyhydrogel form prepared through wet interaction technique was found to be suitable for making low expansion ceramics. ZrO_2 as an additive exhibited positive influence on the sintering of the lithium aluminosilicate powder precursors. For the LAS

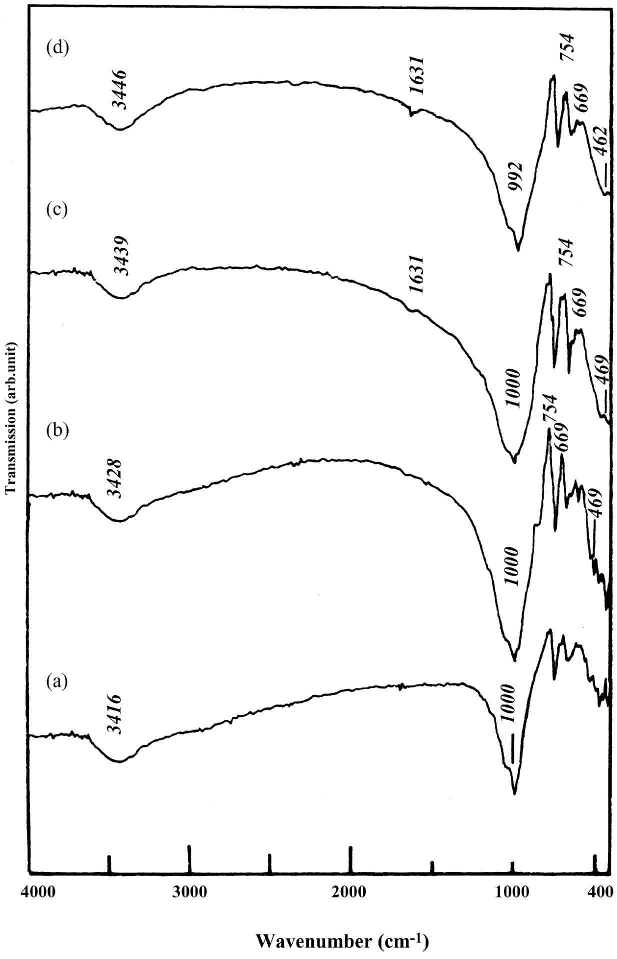

Fig. 8. IR spectra of the samples heat treated at 1300 °C [a: sample I, b: sample II, c: sample III and d: sample IV].

powder precursors containing no ZrO_2 (sample I), the only major crystalline phase obtained was β-spodumene, lithium aluminate and trace amount of β-eucryptite of different crystalline geometry. β-Eucryptite crystalline phase was found to be formed distinctly even at a temperature of 750 °C for samples II–IV and the content increases with increasing sintering temperature. The formation of β-eucryptite in the present system was further supported by their thermal expansion values. The IR results indicated the presence of some residual hydroxy linkages. Zirconia had a dominating influence towards the formation of β-eucryptite in the present system and it not only induces the formation of β-eucryptite but also changes the grain size. A porous low expansion ceramic monolith could be prepared using the present technique.

Acknowledgements

The authors are thankful to Dr. B. Karmakar, Scientist Glass Technology Division for carrying out the IR studies. Thanks are also due to Shri Raj Kumar Mallick, Technical Officer of Refractory Division for carrying out the thermal expansion measurement and to XRD Section, SEM-ESCA Section and Analytical Chemistry Section for their effective assistance.

References

[1] H. Scheidler, E. Rodek, Li_2O–Al_2O_3–SiO_2 glass-ceramics, Am. Ceram. Soc. Bull. 68 (1989) 1926–1930.

[2] M.C. Wang, N.-C. Wu, S. Young, S.-B. Wen, Effect of LiF addition on the phase transition of sinterable β-spodumene precursor powders prepared by a sol–gel process, J. Mater. Res. 17 (8) (2002) 1960–1968.

[3] A. Nordmann, Y.-B. Cheng, Formation and stability of β-quartz solid solution phase in the Li–Al–Si–O–N system, J. Am. Ceram. Soc. 80 (1997) 3045–3053.

[4] A. Nordmann, Y.-B. Cheng, Crystallization behaviour and microstructural evolution of a Li_2O–Al_2O_3–SiO_2 glass derived from spodumene mineral, J. Mater. Sci. 32 (1997) 83–89.

[5] M. Stefano, B. Alessandro, L. Elio, B. Sergio, Synthesis, sintering and thermal expansion of porous low expansion ceramics, J. Eur. Ceram. Soc. 24 (2004) 3535–3540.

[6] J.-K. Yang, S. Sakka, T. Yoko, H. Kozuka, Preparation of lithium aluminosilicate glass ceramic monoliths from metal alkoxide solution: Part II: conversion of gel to glass-ceramic monoliths and their properties, J. Mater. Sci. 26 (1991) 1827–1833.

[7] D.U. Tulyaganov, S. Agathopoulos, H.R. Fernandes, J.M.F. Ferreira, Synthesis of lithium aluminosilicate glass and glass-ceramics from spodumene mineral, Ceram. Int. 30 (2004) 1023–1030.

[8] M.C. Wang, Preparation and characterization of β-spodumene powders by sol–gel process, J. Ceram. Soc. Jpn. 102 (1994) 109–113.

[9] R. Roy, D.K. Agrawal, H.A. Mckinstry, Very low thermal expansion coefficient materials, Annu. Rev. Mater. Sci. 19 (1989) 59–81.

[10] Z. Strand, Glass-Ceramic Materials: Glass Science & Technology 8, Elsevier Science Publishing Company, Inc., New York, 1986 , pp. 85–97.

[11] P.W. Mcmillan, Glass-Ceramics, second ed., Academic Press Inc., New York, 1979, pp. 222–245.

[12] G.H. Beall, Design and properties of glass-ceramics, Annu. Rev. Mater. Sci. 22 (1992) 98.

[13] J. Hlavac, The Technology of Glass and Ceramics: An Introduction: Glass Science & Technology 4, Elsevier Scientific Publishing Company, New York, 1983, pp. 228–237.

[14] G. Orcel, L.L. Hench, in: L.L. Hench, D.R. Ulrich (Eds.), Science of Ceramic Chemical Processing, Wiley Publishing Company, New York, 1986, p. 224.

[15] M.C. Wang, N.-C. Wu, S. Yang, S.-B. Wen, Effect of LiF addition on the phase transition of sinterable β-spodumene precursor powders prepared by a sol–gel process, J. Mater. Res. 17 (8) (2002) 1960–1968.

[16] M.C. Wang, N.-C. Wu, S. Yang, S.-B. Wen, A sintering study on the β-spodumene based glass-ceramics prepared from gel derived precursor powders with LiF additive, Metallurg. Mater. Transact. A: Phys. Metallurg. Mater. Sci. 33 (2002) 171–181.

[17] G.H. Beall, Design and properties of glass-ceramics, Annu. Rev. Mater. Sci. 22 (1992) 91–119.

[18] W.I. Abdel-Fattah, R. Abdellah, Lithia porcelains as promising breeder candidates–I. Preparation and characterization of β-eucryptite and β-spodumene porcelain, Ceram. Int. 23 (1997) 463–469.

[19] M.C. Wang, The effect of TiO_2 addition on the thermal behaviour of sol–gel derived β-spodumene powders, J. Ceram. Soc. Jpn. 10 (1994) 18–23.

[20] A.K. Samanta, K.K. Dhargupta, S. Ghatak, Prevention of oxidation of SiC through reaction bonding in the SiC–mullite composite system by using technique of intermediate gel formation, Trans. Ind. Ceram. Soc. 57 (4) (1998) 103–105.

[21] A.K. Samanta, K.K. Dhargupta, S. Ghatak, Near net shape SiC–mullite composites from a powder precursor prepared through an intermediate Al–hydroxy-hydrogel, Ceram. Int. 27 (2001) 195–199.

[22] A.K. Samanta, K.K. Dhargupta, A.K. De, S. Ghatak, SiC–YAG sintered composites from hydroxy-hydrogel powder precursors, Ceram. Int. 26 (2001) 831–838.

[23] S. Mandal, S. Chakrabarti, S. Das, S. Ghatak, Indian Patent Application for a Process of Preparation of Lithium Aluminosilicate, NF 416/2000 dated 26.12.2002.

[24] S. Mandal, S. Chakrabarti, S. Ghatak, Preparation and characterization of a powder precursor, consisting oxides of Li–Al–Si in the form of hydroxyhydrogel for synthesis of β-spodumene ceramics, Ceram. Int. 30 (3) (2004) 357–367.

[25] S. Mandal, S. Chakrabarti, S. Das, S. Ghatak, Sintering characteristics of in situ formed low expansion ceramics from a powder precursor in the form of hydroxyhydrogel, Ceram. Int. 30 (8) (2004) 2147–2155.

[26] N.S. Akhmetov, General and Inorganic Chemistry, Mir Publishers, Moscow, 1987, pp. 465–57.

[27] F.A. Cotton, G. Wilkinson, Advanced Inorganic Chemistry: A Comprehensive Text, 2nd revision, Wiley Eastern Private Ltd., 1972.

[28] A.K. Samanta, K.K. Dhargupta, S. Ghatak, Retension of SiC during development of SiC–Mx Siy Oz composites (M = Al, Zr, Mg) by reaction bonding in air, J. Eur. Ceram. Soc. 20 (2000) 1883–1894.

[29] Anon, Phase diagrams for ceramists, Am. Ceram. Soc. (1964) 167.

[30] V.W. Sack, H. Scheidler, Glastech. Ber. 39 (1966) 126.

[31] F.A. Wells, Structural Inorganic Chemistry, third ed., Oxford, 1962, p. 457.